Frontiers of Information Technology & Electronic Engineering
www.jzus.zju.edu.cn; engineering.cae.cn; www.springerlink.com
ISSN 2095-9184 (print); ISSN 2095-9230 (online)
E-mail: jzus@zju.edu.cn

Passive source localization using importance sampling based on TOA and FOA measurements*

Rui-rui LIU, Yun-long WANG†‡, Jie-xin YIN, Ding WANG, Ying WU

(*National Digital Switching System Engineering & Technology Research Center, Zhengzhou 450001, China*)

†E-mail: chriswayulo@sina.com

Received Oct. 25, 2016; Revision accepted Apr. 17, 2017; Crosschecked Aug. 18, 2017

Abstract: Passive source localization via a maximum likelihood (ML) estimator can achieve a high accuracy but involves high calculation burdens, especially when based on time-of-arrival and frequency-of-arrival measurements for its internal nonlinearity and nonconvex nature. In this paper, we use the Pincus theorem and Monte Carlo importance sampling (MCIS) to achieve an approximate global solution to the ML problem in a computationally efficient manner. The main contribution is that we construct a probability density function (PDF) of Gaussian distribution, which is called an important function for efficient sampling, to approximate the ML estimation related to complicated distributions. The improved performance of the proposed method is attributed to the optimal selection of the important function and also the guaranteed convergence to a global maximum. This process greatly reduces the amount of calculation, but an initial solution estimation is required resulting from Taylor series expansion. However, the MCIS method is robust to this prior knowledge for point sampling and correction of importance weights. Simulation results show that the proposed method can achieve the Cramér-Rao lower bound at a moderate Gaussian noise level and outperforms the existing methods.

Key words: Passive source localization; Time of arrival (TOA); Frequency of arrival (FOA); Monte Carlo importance sampling (MCIS); Maximum likelihood (ML)

http://dx.doi.org/10.1631/FITEE.1601657 **CLC number:** TN91

1 Introduction

Passive source localization has been a considerable research topic in sensor networks in the signal processing field due to its wide application in target tracking, surveillance, navigation, and wireless communication (Rappaport *et al.*, 1996; Patwari *et al.*, 2005; Dong, 2012). There are various common metrics employed to determine the position of a radiating source, such as received signal strength (RSS) (Weiss, 2003), direction of arrival (DOA) (Yin *et al.*, 2014; 2016), time delay (Knapp and Carter, 1976; Cheung *et al.*, 2004; Chan *et al.*, 2006; Beck *et al.*, 2008; Ma and Ho, 2011; Shen *et al.*, 2012), Doppler-shift, and joint of multiple metrics (Fu *et al.*, 2015; Wang and Wu, 2016).

The RSS localization system determines the target using the received signal power, whose accuracy is limited in complicated, long-distance circumstances because of fading wireless signals (Weiss, 2003). DOA localization is also called angle-of-arrival (AOA) localization, where an antenna array is used to measure the bearing of the source and the localization accuracy decreases rapidly for far-field sources (Yin *et al.*, 2014; 2016). Localization using time delay can obtain excellent accuracy if combined with high efficient time-domain estimate techniques (Knapp and Carter, 1976), which are based on measuring the time of arrival (TOA) or time difference of arrival (TDOA) of the source signal at a few sensors

‡ Corresponding author

* Project supported by the National Natural Science Foundation of China (No. 61201381) and the China Postdoctoral Science Foundation (No. 2016M592989)

ORCID: Rui-rui LIU, http://orcid.org/0000-0002-8870-5237

(Cheung *et al.*, 2004; Chan *et al.*, 2006; Beck *et al.*, 2008; Ma and Ho, 2011; Shen *et al.*, 2012). If there is relative motion between the radiating source and the sensors, the frequency of arrival (FOA) and frequency difference of arrival (FDOA) can be incorporated with the time delay, which can be estimated together (Zhang and Zhang, 2011) to obtain the position and velocity of the source, and to improve the localization accuracy. Although the joint estimation of time delay and Doppler frequency is complicated, the estimate accuracy can be ensured with rapid calculating techniques (Fu *et al.*, 2015; Gu *et al.*, 2017). A number of algorithms have been proposed by Wang and Wu (2016) for TDOA and FDOA localization systems, where relative synchronization between the source and the sensors is unnecessary because of the difference processing. However, the cost of gaining the position and velocity of the reference sensor is high.

As previously mentioned, the localization of a moving source using TOA and FOA measurements is viable when synchronization is achieved and the carrier frequency is available, provided with efficient computation and huge memory (Pan *et al.*, 2016; Xia *et al.*, 2016). It is manifest that this joint localization approach can achieve high accuracy when using the full available information received by all sensors. Recently, TOA and FOA localization approaches have been extensively studied based on communication satellites in geolocation systems (Engel, 2009), because the target can be detected accurately by only two or three satellites and the expense of one satellite is saved compared with TDOA- and FDOA-based localizations. Furthermore, TOA- and FOA-based localizations have been applied in the non-line-of-sight (NLOS) propagation environment (Papakonstantinou and Slock, 2009; Ramlall *et al.*, 2014; Shikur and Weber, 2014). Joint TOA and FOA measurements have also been employed in direct position determination (DPD) techniques, which improves the performance of position determination but the calculation is relatively complicated (Wang and Wu, 2015). However, few algorithms have been developed in universal localization systems for the radiation source. To fill this gap, in this paper we propose a TOA- and FOA-based localization method with higher accuracy, more efficient computation, and greater robustness.

In the TOA and FOA localization system, least squares (LS) or maximum likelihood (ML) estimation can be employed. The LS algorithm needs only to assume a probability model without a probability hypothesis based on the observation data, but the performance is not usually optimal. ML estimation has been verified to be asymptotically unbiased and achieves the Cramér-Rao lower bound (CRLB), and can be applied in source localization (Fletcher and Reeves, 1964; Broyden, 1970; Shanno, 1970; Vandenberghe and Boyd, 1998; Alizadeh and Goldfarb, 2003; Coleman *et al.*, 2006; Elvira *et al.*, 2016). ML estimation of TOA- and FOA-based source localization can be cast as a nonlinear and nonconvex optimization problem, but it is difficult to obtain a global optimal solution. The most direct method is a grid search in the solution space with sufficiently dense grid points. Nevertheless, its computation expense increases exponentially with respect to increased dimensionality. Furthermore, iterative methods can be used to solve the ML problem, and these methods involve searching for the solution of the optimization problem using the initial estimate. The common methods related are the Newton (Broyden, 1970), quasi-Newton (Shanno, 1970), conjugate gradient (Fletcher and Reeves, 1964), and trust region (Coleman *et al.*, 2006) methods. These methods are sensitive to the initial estimate and may converge to a local solution or diverge in high measurement noise. Another available solution is one that relaxes the ML problem to a convex optimization problem, such as semidefinite programming (SDP) (Vandenberghe and Boyd, 1998) and second-order cone programming (SOCP) (Alizadeh and Goldfarb, 2003). More recently, Monte Carlo (MC) techniques have been widely used in signal processing (Huang *et al.*, 2006; Wang and Kay, 2010; Wang and Chen, 2011; Elvira *et al.*, 2016). The most common method is the importance sampling (IS) method, which approximates moments of complicated distributions by drawing samples from a set of proposed distributions (Elvira *et al.*, 2016). Huang *et al.* (2006) used the IS method to solve the ML problem of DOA estimation, reducing the computational complexity of the original maximum likelihood estimate (MLE). Subsequently, a joint angle-Doppler MLE based on the IS technique was proposed (Wang and Kay, 2010), which produces better performance at a low signal-to-noise ratio (SNR) or with a small number of snapshots. Wang and Chen (2011) presented a method for

TDOA-based source localization using the Monte Carlo importance sampling (MCIS) technique to find the approximate global solution to the ML problem. The IS technique can be used to solve TOA- and FOA-based localization because the cost function is a probability density function (PDF) of the measurement noise, and the nonlinear and nonconvex problem of the TOA and FOA equations can be solved efficiently.

In this paper, a high accuracy and low complexity localization approach using both TOA and FOA measurements is presented, which extends the work of Wang and Chen (2011) based on TDOA in line-of-sight (LOS) environments. We formulate an ML estimation of the position and velocity of the source when the measurement noise has a Gaussian distribution. An approximate global solution can be obtained by calculating multi-dimensional integrals derived from the Pincus theorem (Pincus, 1968), which can be efficiently solved by the MCIS technique. A Gaussian distribution PDF is constructed as the importance function by linearizing the TOA and FOA equations via a Taylor series expansion. This process requires an initial estimate of the source position and velocity, which can be roughly obtained by the improved weighted least squares (WLS) method (Beck *et al.*, 2008). Then the global optimal solution is obtained as the expectation of the estimates of a sufficient number of samples based on the law of large numbers. The results show that the MCIS method can provide the optimum performance and approach the CRLB asymptotically at moderate noise levels without the burden of heavy calculation, and it is extremely robust to the initial estimate, especially when it is repeated two or three times.

In this study, we use the following notations: (1) bold-face lowercase letters and bold-face uppercase letters denote vectors and matrices, respectively; (2) $\mathbf{0}_{N\times n}$ denotes an $N\times n$ all-zero matrix and $\mathbf{0}_n$ denotes an n-dimensional zero vector; (3) $\boldsymbol{I}_N$ represents an n-dimensional identity matrix; (4) '$\cdot$' represents the Hadamard product (multiplied by the corresponding elements); (5) $[\cdot]^{-1}$ is the Moore-Penrose inverse of a matrix; (6) diag($\cdot$) denotes the diagonal matrix equipped with the elements of a vector; (7) blkdiag($\cdot$) represents the block diagonal matrix consisting of the matrix or vector; (8) $\boldsymbol{A}(i,:)$ denotes the ith row vector of matrix $\boldsymbol{A}$.

2 Problem formulation

Consider a network composed of N sensors whose locations and velocities are known, denoted by $\boldsymbol{s}_1, \boldsymbol{s}_2, \ldots, \boldsymbol{s}_N$ and $\dot{\boldsymbol{s}}_1, \dot{\boldsymbol{s}}_2, \ldots, \dot{\boldsymbol{s}}_N$, respectively. The sensors are applied to determine the unknown moving source position $\boldsymbol{x}$ and its velocity $\dot{\boldsymbol{x}}$. The unit for the position is meter, and that for the velocity is m/s. Generally, at least N=2 sensors are required to generate two pairs of TOA and FOA measurements in a two-dimensional (2D) scenario and N=3 in a 3D scenario.

Assumptions are: (1) The sensors are not lying on a plane or a straight line, and this ensures that the TOA and FOA equations are uncorrelated; (2) The localization metrics are line-of-sight (LOS) measurements and we consider only the measurement noise; (3) The measurement noise of TOA and FOA follows a Gaussian distribution, so the cost function can be viewed as a Gaussian-distributed PDF and the proposal importance function is valid.

The LOS TOA of a signal received by sensor i is given by

$$\tau_i = \frac{1}{c}\left\|\boldsymbol{x}-\boldsymbol{s}_i\right\|,\ i=1,2,\ldots,N, \tag{1}$$

where c is the signal propagation speed. Multiplying both sides of the TOA equation by c in Eq. (1), the range of arrival (ROA) can be obtained as

$$d_i = c\tau_i = \|\boldsymbol{x}-\boldsymbol{s}_i\|,\ i=1,2,...,N. \tag{2}$$

The derivative of Eq. (2) gives the relationship between the range rates:

$$\dot{d}_i = \frac{(\dot{\boldsymbol{x}}-\dot{\boldsymbol{s}}_i)^{\mathrm{T}}(\boldsymbol{x}-\boldsymbol{s}_i)}{\|\boldsymbol{x}-\boldsymbol{s}_i\|},\ i=1,2,...,N, \tag{3}$$

where $(\cdot)^{\mathrm{T}}$ represents the transpose of a matrix.

Let z_i and $\dot{z}_i$ be the measurements of the noise range and noise range rate, respectively. The TOA and FOA measurements can be described by the additive noise model as

$$\begin{cases} z_i = \|\boldsymbol{x}-\boldsymbol{s}_i\| + e_i = d_i + e_i, \\ \dot{z}_i = \dfrac{(\dot{\boldsymbol{x}}-\dot{\boldsymbol{s}}_i)^{\mathrm{T}}(\boldsymbol{x}-\boldsymbol{s}_i)}{\|\boldsymbol{x}-\boldsymbol{s}_i\|} + \dot{e}_i = \dot{d}_i + \dot{e}_i, \end{cases} \quad i=1,2,\cdots,N, \tag{4}$$

where e_i and $\dot{e}_i$ denote the TOA and FOA measurement noises, respectively.

Denote $\boldsymbol{z}=[z_1, z_2, \ldots, z_N]^{\mathrm{T}}$, $\dot{\boldsymbol{z}}=[\dot{z}_1,\dot{z}_2,...,\dot{z}_N]^{\mathrm{T}}$, $\boldsymbol{d}=[d_1, d_2, \ldots, d_N]^{\mathrm{T}}$, $\dot{\boldsymbol{d}}=[\dot{d}_1,\dot{d}_2,...,\dot{d}_N]^{\mathrm{T}}$, $\boldsymbol{e}=[e_1, e_2, \ldots, e_N]^{\mathrm{T}}$, and $\dot{\boldsymbol{e}}=[\dot{e}_1,\dot{e}_2,...,\dot{e}_N]^{\mathrm{T}}$. Accordingly, we can rewrite TOA and FOA measurements in Eq. (4) in the following vector form:

$$\begin{cases}\boldsymbol{z}=\boldsymbol{d}+\boldsymbol{e},\\ \dot{\boldsymbol{z}}=\dot{\boldsymbol{d}}+\dot{\boldsymbol{e}}.\end{cases} \tag{5}$$

3 Localization using importance sampling

Given that MLE (Kay, 1993) has been verified as asymptotically unbiased and can achieve the CRLB, it can be employed to solve TOA- and FOA-based localization problems under the Gaussian distributed measurement noise.

Based on Eq. (5), the ML estimation of the source location and velocity $\boldsymbol{\theta}=[\boldsymbol{x}^{\mathrm{T}}, \dot{\boldsymbol{x}}^{\mathrm{T}}]^{\mathrm{T}}$ can be formulated by

$$\min_{\boldsymbol{\theta}} f(\boldsymbol{\theta})=\tilde{\boldsymbol{e}}^{\mathrm{T}}\boldsymbol{Q}^{-1}\tilde{\boldsymbol{e}}=(\tilde{\boldsymbol{z}}-\tilde{\boldsymbol{d}})^{\mathrm{T}}\boldsymbol{Q}^{-1}(\tilde{\boldsymbol{z}}-\tilde{\boldsymbol{d}}), \tag{6}$$

where $\tilde{\boldsymbol{z}}=[\boldsymbol{z}^{\mathrm{T}},\dot{\boldsymbol{z}}^{\mathrm{T}}]^{\mathrm{T}}$, $\tilde{\boldsymbol{e}}=[\boldsymbol{e}^{\mathrm{T}},\dot{\boldsymbol{e}}^{\mathrm{T}}]^{\mathrm{T}}$, $\tilde{\boldsymbol{d}}=[\boldsymbol{d}^{\mathrm{T}},\dot{\boldsymbol{d}}^{\mathrm{T}}]^{\mathrm{T}}$, $\boldsymbol{Q}_{\mathrm{e}}=E[\boldsymbol{e}\boldsymbol{e}^{\mathrm{T}}]$, $\dot{\boldsymbol{Q}}_{\mathrm{e}}=E[\dot{\boldsymbol{e}}\dot{\boldsymbol{e}}^{\mathrm{T}}]$, and $\boldsymbol{Q}=\mathrm{blkdiag}(\boldsymbol{Q}_{\mathrm{e}},\dot{\boldsymbol{Q}}_{\mathrm{e}})$.

3.1 Global solution to ML estimation

In this section, we transform ML estimation into a multidimensional optimization problem, which can be efficiently solved by the Pincus theorem (Pincus, 1968). We introduce it as follows:

Theorem 1 Let $F(z_1, z_2, \ldots, z_n)=F(\boldsymbol{z})$ be a continuous function on a bounded domain $\mathbb{S}$ in n-dimensional Euclidean space $\mathbb{R}^n$. Assume that $F(\boldsymbol{z})$ attains a global maximum at an exact point $\hat{\boldsymbol{z}}=[\hat{z}_1,\hat{z}_2,...,\hat{z}_n]^{\mathrm{T}}$ of $\mathbb{S}$. Then for $i=1, 2, \ldots, n$,

$$\hat{z}_i=\lim_{\lambda\to\infty}\frac{\int\int\cdots\int_S z_i\exp[\lambda F(\boldsymbol{z})]\mathrm{d}z_1\mathrm{d}z_2\cdots\mathrm{d}z_n}{\int\int\cdots\int_S\exp[\lambda F(\boldsymbol{z})]\mathrm{d}z_1\mathrm{d}z_2\cdots\mathrm{d}z_n}. \tag{7}$$

According to Theorem 1, we assume that $f(\boldsymbol{\theta})$ attains a global minimum at an exact point $\hat{\boldsymbol{\theta}}=[\hat{\theta}_1,\hat{\theta}_2,\ldots,\hat{\theta}_n]^{\mathrm{T}}$ of $\mathbb{S}$, which is given by

$$\hat{\theta}_i=\lim_{\lambda\to\infty}\frac{\int\int\cdots\int_S\theta_i\exp[-\lambda f(\boldsymbol{\theta})]\mathrm{d}\theta_1\mathrm{d}\theta_2\cdots\mathrm{d}\theta_n}{\int\int\cdots\int_S\exp[-\lambda f(\boldsymbol{\theta})]\mathrm{d}\theta_1\mathrm{d}\theta_2\cdots\mathrm{d}\theta_n},\quad i=1,2,\ldots,n. \tag{8}$$

In actual TOA and FOA measurements, we can determine a sufficiently large domain where $\boldsymbol{\theta}$ lies based on the radio range of sensors to guarantee that $\boldsymbol{\theta}$ is in a bounded domain.

Define a function $p(\boldsymbol{\theta})$ as

$$p(\boldsymbol{\theta})=\frac{\exp[-\lambda f(\boldsymbol{\theta})]}{\int\int\cdots\int\exp[-\lambda f(\boldsymbol{\theta})]\mathrm{d}\theta_1\mathrm{d}\theta_2\cdots\mathrm{d}\theta_n}. \tag{9}$$

Note that $p(\boldsymbol{\theta})$ in Eq. (9) has all the properties of a PDF. Therefore, we might consider $p(\boldsymbol{\theta})$ as a pseudo-PDF of random vector $\boldsymbol{\theta}$.

Based on the above definition and theorem, the global minimum can be computed as the mean of the pseudo-PDF $p(\boldsymbol{\theta})$ as long as λ is large enough, and Eq. (8) can be rewritten as

$$\hat{\theta}_i=\lim_{\lambda\to\infty}\int\theta_i q(\boldsymbol{\theta})\mathrm{d}\theta_1\mathrm{d}\theta_2\cdots\mathrm{d}\theta_n,\ i=1,2,...,n. \tag{10}$$

The calculation of estimator $\hat{\theta}_i$ in Eq. (10) requires M-dimensional integrals, which in general cannot be achieved. Fortunately, we can dispose the complex integrals approximately by the MCIS technique, which is described in Section 3.2.

3.2 Monte Carlo importance sampling

MCIS has been regarded as a powerful tool to compute a multidimensional integral in the following form:

$$I=\int h(\boldsymbol{\theta})p(\boldsymbol{\theta})\mathrm{d}\boldsymbol{\theta}. \tag{11}$$

Assuming that $q(\boldsymbol{\theta})$ is a PDF with respect to $\boldsymbol{\theta}$, the integral in Eq. (11) can be expressed as the expected value of $h(\boldsymbol{\theta})w(\boldsymbol{\theta})$ with respect to $q(\boldsymbol{\theta})$:

$$I=\int h(\boldsymbol{\theta})w(\boldsymbol{\theta})q(\boldsymbol{\theta})\,\mathrm{d}\boldsymbol{\theta}=\mathbb{E}_q[h(\boldsymbol{\theta})w(\boldsymbol{\theta})], \quad (12)$$

where $q(\boldsymbol{\theta})$ is defined as an importance function and $w(\boldsymbol{\theta})=p(\boldsymbol{\theta})/q(\boldsymbol{\theta})$ is the importance weight.

According to the law of large numbers and $\int w(\boldsymbol{\theta})q(\boldsymbol{\theta})\,\mathrm{d}\boldsymbol{\theta}=1$, the expected value can be expressed as

$$\begin{aligned}\mathbb{E}_q\left[h(\boldsymbol{\theta})w(\boldsymbol{\theta})\right]&=\frac{\int h(\boldsymbol{\theta})w(\boldsymbol{\theta})q(\boldsymbol{\theta})\mathrm{d}\boldsymbol{\theta}}{\int w(\boldsymbol{\theta})q(\boldsymbol{\theta})\mathrm{d}\boldsymbol{\theta}}\\&=\lim_{M\to\infty}\frac{\frac{1}{M}\sum_{m=1}^{M}h(\boldsymbol{\theta}_m)w(\boldsymbol{\theta}_m)}{\frac{1}{M}\sum_{m=1}^{M}w(\boldsymbol{\theta}_m)}\\&\doteq\sum_{m=1}^{M}h(\boldsymbol{\theta}_m)\tilde{w}(\boldsymbol{\theta}_m),\end{aligned} \quad (13)$$

where $\boldsymbol{\theta}_m$ is drawn according to $q(\boldsymbol{\theta})$ in M sampling points and the normalized importance weight $\tilde{w}(\boldsymbol{\theta}_m)$ is given by

$$\tilde{w}(\boldsymbol{\theta}_m)=\frac{w(\boldsymbol{\theta}_m)}{\sum_{m=1}^{M}w(\boldsymbol{\theta}_m)}. \quad (14)$$

3.3 Choice of the importance function for TOA- and FOA-based localizations

If we can find an importance function $q(\boldsymbol{\theta})$ to approximate $p(\boldsymbol{\theta})$ in Eq. (9), $\boldsymbol{\theta}_m$ can be drawn from $q(\boldsymbol{\theta})$ directly to calculate the integration. Since the Gaussian distribution has an extensive practical background and is subject only to the mean and covariance, which can be constructed easily, we construct $q(\boldsymbol{\theta})$ as a Gaussian distributed PDF.

Note that Eq. (4) is equivalent to

$$\begin{cases}z_i-\|\boldsymbol{x}-\boldsymbol{s}_i\|=e_i,\\ \dot{z}_i-\dfrac{(\dot{\boldsymbol{x}}-\dot{\boldsymbol{s}}_i)^{\mathrm{T}}(\boldsymbol{x}-\boldsymbol{s}_i)z_i}{\|\boldsymbol{x}-\boldsymbol{s}_i\|}=\dot{e}_i,\end{cases}\quad i=1,2,\ldots,N. \quad (15)$$

Assuming that initial estimates of the source location and velocity are available, denoted by $\boldsymbol{x}^*$ and $\dot{\boldsymbol{x}}^*$, respectively, we approximate TOAs and FOAs via their first-order Taylor series expansions, leading to the following formulations:

$$e_i\doteq-\frac{(\boldsymbol{x}^*-\boldsymbol{s}_i)^{\mathrm{T}}}{d_i^*}(\boldsymbol{x}-\boldsymbol{x}^*)-d_i^*+z_i, \quad (16)$$

$$\begin{aligned}\dot{e}_i\doteq&\left(\frac{(\dot{\boldsymbol{x}}^*-\dot{\boldsymbol{s}}_i)^{\mathrm{T}}}{d_i^*}-\frac{(\boldsymbol{x}^*-\boldsymbol{s}_i)^{\mathrm{T}}\dot{d}_i^*}{(d_i^*)^2}\right)(\boldsymbol{x}-\boldsymbol{x}^*)\\&-\frac{(\boldsymbol{x}^*-\boldsymbol{s}_i)^{\mathrm{T}}}{d_i^*}(\dot{\boldsymbol{x}}-\dot{\boldsymbol{x}}^*)-\dot{d}_i^*+\dot{z}_i,\end{aligned} \quad (17)$$

where $d_i^*=\|\boldsymbol{x}^*-\boldsymbol{s}_i\|$ and $\dot{d}_i^*=\dfrac{(\dot{\boldsymbol{x}}^*-\dot{\boldsymbol{s}}_i)^{\mathrm{T}}(\boldsymbol{x}^*-\boldsymbol{s}_i)}{\|\boldsymbol{x}^*-\boldsymbol{s}_i\|}$.

Note that e_i is a linear function of $\boldsymbol{x}$, and $\dot{e}_i$ is also a linear function of $\boldsymbol{x}$ and $\dot{\boldsymbol{x}}$, in Eqs. (16) and (17). We can rewrite Eqs. (16) and (17) in the following matrix form:

$$\begin{cases}\boldsymbol{e}\doteq\boldsymbol{B}\boldsymbol{x}-\boldsymbol{b},\\ \dot{\boldsymbol{e}}\doteq\boldsymbol{H}\boldsymbol{x}+\boldsymbol{F}\dot{\boldsymbol{x}}-\boldsymbol{h},\end{cases} \quad (18)$$

where

$$\begin{aligned}\boldsymbol{B}&=-\begin{bmatrix}\dfrac{(\boldsymbol{x}^*-\boldsymbol{s}_1)^{\mathrm{T}}}{d_1^*}\\ \vdots\\ \dfrac{(\boldsymbol{x}^*-\boldsymbol{s}_N)^{\mathrm{T}}}{d_N^*}\end{bmatrix},\boldsymbol{b}=-\begin{bmatrix}z_1-d_1^*+\dfrac{(\boldsymbol{x}^*-\boldsymbol{s}_1)^{\mathrm{T}}}{d_1^*}\boldsymbol{x}^*\\ \vdots\\ z_N-d_N^*+\dfrac{(\boldsymbol{x}^*-\boldsymbol{s}_N)^{\mathrm{T}}}{d_N^*}\boldsymbol{x}^*\end{bmatrix},\\ \boldsymbol{F}&=\begin{bmatrix}\dfrac{(\boldsymbol{s}_1-\boldsymbol{x}^*)^{\mathrm{T}}}{d_1^*}\\ \vdots\\ \dfrac{(\boldsymbol{s}_N-\boldsymbol{x}^*)^{\mathrm{T}}}{d_N^*}\end{bmatrix},\boldsymbol{H}=\begin{bmatrix}-\boldsymbol{F}(1,:)-\dfrac{(\boldsymbol{x}^*-\boldsymbol{s}_1)^{\mathrm{T}}\dot{d}_1^*}{d_1^{*2}}\\ \vdots\\ -\boldsymbol{F}(N,:)-\dfrac{(\boldsymbol{x}^*-\boldsymbol{s}_N)^{\mathrm{T}}\dot{d}_N^*}{d_N^{*2}}\end{bmatrix},\\ \boldsymbol{h}&=-\begin{bmatrix}(\dot{z}_1-\dot{d}_1^*)-\boldsymbol{H}(1,:)\boldsymbol{x}^*-\boldsymbol{F}(1,:)\dot{\boldsymbol{x}}^*\\ \vdots\\ (\dot{z}_N-\dot{d}_N^*)-\boldsymbol{H}(N,:)\boldsymbol{x}^*-\boldsymbol{F}(N,:)\dot{\boldsymbol{x}}^*\end{bmatrix}.\end{aligned} \quad (19)$$

Combining the two formulas in Eq. (18) yields

$$\boldsymbol{\varepsilon}\doteq\boldsymbol{K}\boldsymbol{\theta}-\boldsymbol{\kappa}, \quad (20)$$

where

$$\boldsymbol{\kappa}=[\boldsymbol{b}^{\mathrm{T}},\boldsymbol{h}^{\mathrm{T}}]^{\mathrm{T}},\ \boldsymbol{\varepsilon}=[\boldsymbol{e}^{\mathrm{T}},\dot{\boldsymbol{e}}^{\mathrm{T}}]^{\mathrm{T}},\ \boldsymbol{K}=\begin{bmatrix}\boldsymbol{B}^{\mathrm{T}} & \boldsymbol{0}_{N\times n}^{\mathrm{T}}\\ \boldsymbol{H}^{\mathrm{T}} & \boldsymbol{F}^{\mathrm{T}}\end{bmatrix}^{\mathrm{T}}. \tag{21}$$

This process guarantees that TOA and FOA measurements can be used cooperatively to estimate the source position and velocity.

Based on Eqs. (6) and (20), the ML estimate can be approximated as

$$f(\boldsymbol{\theta})\doteq(\boldsymbol{K}\boldsymbol{\theta}-\boldsymbol{\kappa})^{\mathrm{T}}\boldsymbol{Q}^{-1}(\boldsymbol{K}\boldsymbol{\theta}-\boldsymbol{\kappa}). \tag{22}$$

Thus, the importance function can be built as

$$q(\boldsymbol{\theta})=\frac{\exp\left[-\lambda_1(\boldsymbol{K}\boldsymbol{\theta}-\boldsymbol{\kappa})^{\mathrm{T}}\boldsymbol{Q}^{-1}(\boldsymbol{K}\boldsymbol{\theta}-\boldsymbol{\kappa})\right]}{\int\exp\left[-\lambda_1(\boldsymbol{K}\boldsymbol{\theta}-\boldsymbol{\kappa})^{\mathrm{T}}\boldsymbol{Q}^{-1}(\boldsymbol{K}\boldsymbol{\theta}-\boldsymbol{\kappa})\right]\mathrm{d}\boldsymbol{x}}, \tag{23}$$

where λ in Eq. (9) is replaced by λ_1 in Eq. (23) to adjust the size of the drawn sampling region.

To construct a Gaussian distributed PDF, manipulations can be given by

$$\begin{aligned}&(\boldsymbol{K}\boldsymbol{\theta}-\boldsymbol{\kappa})^{\mathrm{T}}\boldsymbol{Q}^{-1}(\boldsymbol{K}\boldsymbol{\theta}-\boldsymbol{\kappa})\\&=\left[\boldsymbol{\theta}-(\boldsymbol{K}^{\mathrm{T}}\boldsymbol{Q}^{-1}\boldsymbol{K})^{-1}\boldsymbol{K}^{\mathrm{T}}\boldsymbol{Q}^{-1}\boldsymbol{\kappa}\right]^{\mathrm{T}}(\boldsymbol{K}^{\mathrm{T}}\boldsymbol{Q}^{-1}\boldsymbol{K})\\&\cdot\left[\boldsymbol{\theta}-(\boldsymbol{K}^{\mathrm{T}}\boldsymbol{Q}^{-1}\boldsymbol{K})^{-1}\boldsymbol{K}^{\mathrm{T}}\boldsymbol{Q}^{-1}\boldsymbol{\kappa}\right]\\&+\boldsymbol{\kappa}^{\mathrm{T}}\boldsymbol{Q}^{-1}\boldsymbol{\kappa}-\boldsymbol{\kappa}^{\mathrm{T}}\boldsymbol{Q}^{-1}\boldsymbol{K}(\boldsymbol{K}^{\mathrm{T}}\boldsymbol{Q}^{-1}\boldsymbol{K})^{-1}\boldsymbol{K}^{\mathrm{T}}\boldsymbol{Q}^{-1}\boldsymbol{\kappa}\\&=(\boldsymbol{\theta}-\overline{\boldsymbol{\theta}})^{\mathrm{T}}\boldsymbol{R}^{-1}(\boldsymbol{\theta}-\overline{\boldsymbol{\theta}})+\gamma,\end{aligned} \tag{24}$$

where

$$\begin{cases}\overline{\boldsymbol{\theta}}=(\boldsymbol{K}^{\mathrm{T}}\boldsymbol{Q}^{-1}\boldsymbol{K})^{-1}\boldsymbol{K}^{\mathrm{T}}\boldsymbol{Q}^{-1}\boldsymbol{\kappa},\\ \boldsymbol{R}=(\boldsymbol{K}^{\mathrm{T}}\boldsymbol{Q}^{-1}\boldsymbol{K})^{-1},\\ \gamma=\boldsymbol{\kappa}^{\mathrm{T}}\boldsymbol{Q}^{-1}\boldsymbol{\kappa}-\boldsymbol{\kappa}^{\mathrm{T}}\boldsymbol{Q}^{-1}\boldsymbol{K}(\boldsymbol{K}^{\mathrm{T}}\boldsymbol{Q}^{-1}\boldsymbol{K})^{-1}\boldsymbol{K}^{\mathrm{T}}\boldsymbol{Q}^{-1}\boldsymbol{\kappa}.\end{cases} \tag{25}$$

Substituting Eq. (24) into Eq. (23) yields

$$q(\boldsymbol{\theta})=\frac{\exp\left[-\lambda_1(\boldsymbol{\theta}-\overline{\boldsymbol{\theta}})^{\mathrm{T}}\boldsymbol{R}^{-1}(\boldsymbol{\theta}-\overline{\boldsymbol{\theta}})\right]}{\int\exp\left[-\lambda_1(\boldsymbol{\theta}-\overline{\boldsymbol{\theta}})^{\mathrm{T}}\boldsymbol{R}^{-1}(\boldsymbol{\theta}-\overline{\boldsymbol{\theta}})\right]\mathrm{d}\boldsymbol{\theta}}, \tag{26}$$

where $\exp(-\lambda_1\gamma)$ is eliminated and the denominator $\int\exp[-\lambda_1(\boldsymbol{\theta}-\overline{\boldsymbol{\theta}})^{\mathrm{T}}\boldsymbol{R}^{-1}(\boldsymbol{\theta}-\overline{\boldsymbol{\theta}})]\mathrm{d}\boldsymbol{\theta}=(2\pi)^{N/2}\left|\boldsymbol{R}/(2\lambda_1)\right|^{N/2}$.

Hence, $q(\boldsymbol{\theta})$ can be rewritten as

$$q(\boldsymbol{\theta})=\frac{\exp\left[-\lambda_1(\boldsymbol{\theta}-\overline{\boldsymbol{\theta}})^{\mathrm{T}}\boldsymbol{R}^{-1}(\boldsymbol{\theta}-\overline{\boldsymbol{\theta}})\right]}{(2\pi)^{N/2}\left|\boldsymbol{R}/(2\lambda_1)\right|^{1/2}}. \tag{27}$$

Note that function $q(\boldsymbol{\theta})$ has the properties of a Gaussian distribution PDF with mean $\overline{\boldsymbol{\theta}}$ and covariance $\boldsymbol{R}/(2\lambda_1)$. The established forms of $\overline{\boldsymbol{\theta}}$ and $\boldsymbol{R}/(2\lambda_1)$ in Eq. (25) reveal that they are actually the linear WLS estimates, and the covariance is just a constraint to λ_1. It is observed that λ_1 determines the amplitude and width of the Gaussian distribution PDF, and then impacts the dispersion degree of the samples. Intuitively, if λ_1 is too large, the importance function will be too narrow to generate a sufficient number of possible values close to the global optimum. On the other hand, a small value of λ_1 will shape a broad PDF that generates samples far from the global optimum. Given this, we choose λ_1=0.5 and the optimal choice of λ_1 will be further discussed in Section 4. Fortunately, extensive simulations indicate that the estimation performance is almost independent of λ_1.

3.4 Estimation of source positon and velocity

Since the importance function $q(\boldsymbol{\theta})$ has been constructed based on Eq. (27), the ML estimates for position and velocity are readily obtained by

$$\hat{\boldsymbol{\theta}}=\sum_{m=1}^{M}\boldsymbol{\theta}_m\tilde{w}(\boldsymbol{\theta}_m), \tag{28}$$

where $\tilde{w}(\boldsymbol{\theta}_m)=w(\boldsymbol{\theta}_m)\Big/\sum_{m=1}^{M}w(\boldsymbol{\theta}_m)$ with $w(\boldsymbol{\theta}_m)=p(\boldsymbol{\theta}_m)/q(\boldsymbol{\theta}_m)$ and $\boldsymbol{\theta}_m$ is the mth sample drawn according to $q(\boldsymbol{\theta})$.

Note that the denominators in Eq. (22) and the multiplier in Eq. (27) are constants, which can be eliminated by normalization. Thus, $w(\boldsymbol{\theta}_m)$ can be simplified into the following form:

$$w(\boldsymbol{\theta}_m)=\exp\left[-\lambda f(\boldsymbol{\theta}_m)-\lambda_1(\boldsymbol{\theta}_m-\overline{\boldsymbol{\theta}})^{\mathrm{T}}\boldsymbol{R}^{-1}(\boldsymbol{\theta}_m-\overline{\boldsymbol{\theta}})\right]. \tag{29}$$

From the above equations, the importance weights, which are exponential, may generate very small values because $f(\boldsymbol{\theta}_m)$ is always nonnegative. To alleviate this difficulty, we normalize the importance

weight as

$$w'(\boldsymbol{\theta}_m)=\exp\Big[-\lambda f(\boldsymbol{\theta}_m)-\lambda_1(\boldsymbol{\theta}_m-\bar{\boldsymbol{\theta}})^{\mathrm{T}}\boldsymbol{R}^{-1}(\boldsymbol{\theta}_m-\bar{\boldsymbol{\theta}}) - \max_{1\le m\le M}(-\lambda f(\boldsymbol{\theta}_m)-\lambda_1(\boldsymbol{\theta}_m-\bar{\boldsymbol{\theta}})^{\mathrm{T}}\boldsymbol{R}^{-1}(\boldsymbol{\theta}_m-\bar{\boldsymbol{\theta}}))\Big]. \tag{30}$$

To obtain the normalized importance weight $w'(\boldsymbol{\theta}_m)$, the choice of λ should be taken into consideration. In Pincus theory, the global optimum can be obtained when $\lambda\to\infty$, but this is impossible to achieve in practice. However, we can approximate λ by a sufficiently large value to meet the above condition. The simulations in Section 4 will verify the feasibility of this approximation, and the results show that the performance of the MCIS method is almost independent of λ as long as it is large enough.

3.5 Summary of steps

We summarize the implementation procedure of the MCIS method as follows:

1. Find the coefficient matrices $\boldsymbol{B}$, $\boldsymbol{H}$, and $\boldsymbol{F}$ and vectors $\boldsymbol{b}$ and $\boldsymbol{h}$ in Eq. (19) using $\boldsymbol{x}^*$ and $\dot{\boldsymbol{x}}^*$ derived from the improved WLS method, and calculate the joint coefficient matrix $\boldsymbol{K}$ in Eq. (21).

2. Compute the mean value $\bar{\boldsymbol{\theta}}$ and covariance matrix $\boldsymbol{R}$ in Eq. (24) to construct the importance function $q(\boldsymbol{\theta})$ of the Gaussian distribution in Eq. (27).

3. Let λ_1=0.5, set the number of sampling points M=50, and use the probability integral transformation theorem (Kay, 2006) to generate the realization of $\boldsymbol{\theta}_m$ (m=1, 2, …, M). To do this, generate M independent and identically distributed random vectors $\boldsymbol{u}_m$ from a uniform distribution on [0, 1].

4. For each $\boldsymbol{u}_i$, find the value in $q(\boldsymbol{\theta})$ closest to $\boldsymbol{u}_i$ and yield the realization $\boldsymbol{\theta}_i=q(u_i)$.

5. Compute $w'(\boldsymbol{\theta}_m)$ in Eq. (30) and estimate $\hat{\boldsymbol{\theta}}$ using Eq. (31):

$$\hat{\boldsymbol{\theta}}=\sum_{m=1}^{M}\boldsymbol{\theta}_m\frac{w'(\boldsymbol{\theta}_m)}{\sum_{m=1}^{M}w'(\boldsymbol{\theta}_m)}. \tag{31}$$

Here, we have to illustrate the improved WLS method inspired by Beck *et al.* (2008), where a least squares method is applied to the squared range measurements. This method can be directly applied in TOA measurements which are equivalent to range measurements, and a little improvement in FOA measurements will coordinate with TOA measurements for localization. This improved WLS method can give a closed-form solution with insignificant calculation. Although this method encounters a loss of localization accuracy, it can give an initial estimate for the MCIS method.

If the measurement noise is high in severe environments, the proposed method may need repetitions to improve localization accuracy. Repeating the solution computation one or two times is sufficient to yield an accurate solution that reaches CRLB for Gaussian noise.

3.6 Complexity analysis

We compare the complexity of the proposed MCIS method with those of the improved WLS, the Taylor series (Foy, 1976), and the grid search methods in Table 1.

Table 1 Complexity assessment of the existing algorithms

Algorithm	Complexity	CR	RT (s)
MCIS	$O(20NK+10K^2+2MK+MN^2)$	1.0000	1.012
WLS	$O(20NK+2K^2+N^2)$	0.1916	0.656
TS	$O((20NK+4K^2+N^2)N_{\mathrm{Itr}})$	4.0839	1.690
GS	$O((2NK+4K^2)N_{\mathrm{grid}}^{2K})$	6559.0000	53.631

TS: Taylor series; GS: grid search. CR: complexity ratio; RT: running time. N: number of sensors; K: dimensionality of the estimation; M: number of sampling points; N_{Itr}: number of iterations in the iterative method; N_{grid}: number of grids used in the grid search method

As for the proposed method, the complexity of each importance sampling is $O(N^2)$, and the complexity is $O(MN^2)$ when we draw M samples (Wang and Chen, 2011). Typically, M is set at 50–150, which is large enough for sufficient estimation accuracy. The improved WLS method has a closed-form solution, whose complexity is the smallest. The complexity of localization using the Taylor series interior point method is related to the number of iterations N_{Itr}. If we apply a grid search to solve the MLE problem directly, the complexity relates to the grid number N_{grid} and jumps exponentially with dimensionality K. Specifically, we examine the complexity ratio and running time among these four methods in Table 1, suggesting that the MCIS method is more computationally modest than the Taylor series and grid search methods (Wang *et al.*, 2008; Masmoudi *et al.*, 2013).

4 Simulation results

In the following simulations, the proposed method (MCIS) is compared with the Taylor series method (TS) representing the iteration method, and the improved weighted least squares method (WLS) representing the closed-form method.

4.1 Influence on the choice of λ and λ_1

We have briefly illustrated the principle of choosing λ and λ_1 in the previous section. Simulations are conducted to verify the preceding analyses. We consider a 2D scenario with four different sensors, whose locations and velocities are listed in Table 2. There exists a moving source that is located at (600, −50) with velocity (30, −15). The estimation accuracy is evaluated in terms of the root mean square error (RMSE):

$$\mathrm{RMSE}(\boldsymbol{x})=\sqrt{\frac{1}{N}\sum_{n=1}^{N}\|\hat{\boldsymbol{x}}-\boldsymbol{x}\|^2},$$

which are shown in a logarithm scale as the noise power increases (the 10lg(·) operator is used explicitly when position and velocity estimate RMSEs are curved in the same plot). First, we fix λ_1=0.5 and vary λ from 0 to 2000 with an interval of 200. The simulation results are shown in Fig. 1a, from which we can see that the RMSEs of both position and velocity estimates are steady when λ is larger than 200. It is demonstrated that the MCIS method can obtain a global optimum as long as λ is sufficiently large. Then, we vary λ_1 from 0 to 3.5 with an interval of 0.5 when λ=2000. Fig. 1b depicts the RMSEs of position and velocity estimates versus λ_1, and illustrates that the choice of λ_1 has almost no effect on the estimation accuracy of the proposed method. Thus, the settings of λ=2000 and λ_1=0.5 in the following simulations are reasonable and valid.

Table 2 Positions and velocities of sensors in the 2D scenario

Sensor index	Sensor position (m)		Sensor velocity (m/s)	
	x	y	v_x	v_y
1	−300	200	10	−10
2	300	−200	20	10
3	300	200	−10	20
4	−300	−200	15	−15

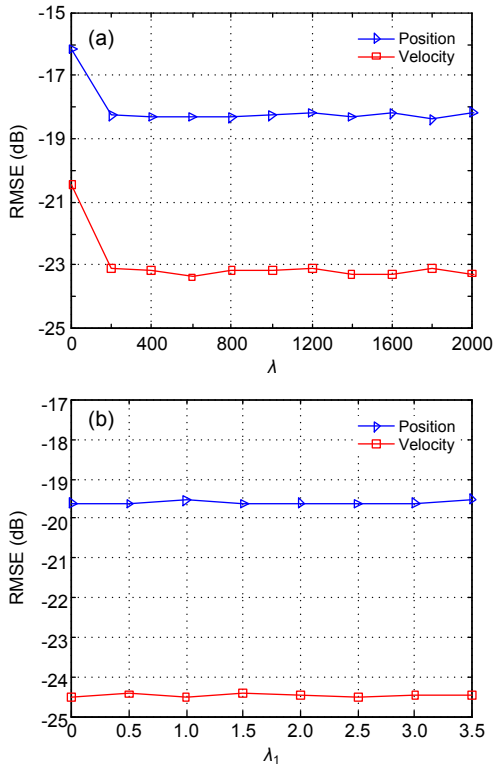

Fig. 1 Sensitivity of RMSEs to λ with λ_1=0.5 (a) and sensitivity of RMSEs to λ_1 with λ=2000 (b)
The passive source is located at (600, −50) with velocity (30, −15)

4.2 Estimation performance of source positon and velocity

In this section, we examine the accuracy of the source position and velocity estimates in two different scenarios.

4.2.1 Two-dimensional scenario

We first consider four sensors in a 2D scenario (Table 2). There exists a moving source that is located at (600, −50) with velocity (30, −15). The TOA and FOA measurements are contaminated by zero-mean Gaussian noise with covariance matrices $\boldsymbol{Q}_e=\sigma_e^2\boldsymbol{R}$ and $\dot{\boldsymbol{Q}}_e=\dot{\sigma}_e^2\boldsymbol{R}$, respectively, where $\boldsymbol{R}$ is equal to unity in the diagonal elements and 0.5 otherwise. σ_e^2 and $\dot{\sigma}_e^2$ are the measurement noise power of TOA and FOA, respectively, and are modified to represent different noise levels. We always claim $\dot{\sigma}_e^2=0.1\sigma_e^2$ because the magnitude of the FOA noise is an order lower than that of the TOA noise in actual measurements.

We conduct 1000 Monte Carlo experiments with M=50 sampling points, which is large enough for a sufficient accuracy. CRLB is also plotted in the figure. Fig. 2a shows the RMSEs of position estimate versus σ_e and Fig. 2b shows the RMSEs of velocity estimates versus σ_e. As shown, all the algorithms attain the CRLB at low noise levels. As the measurement noise increases, the WLS method performs much worse and is the first to exhibit a 'nonlinear threshold phenomenon', the so-called threshold effect. At this point, the localization method based on the analysis of the first-order error will fail and its RMSEs curve deviates from the CRLB. The threshold effect occurs for σ_e=8 in the TS method, because descaling of the second-order items of noises introduces significant errors. More analytically, the threshold of the closed-form method is lower than that of the iterative method, and this is the cost of negligible calculation for the closed-form method. The MCIS method shows performance superior to those of the other two methods and its performance degrades significantly until σ_e increases to 11. It can be interpreted that the importance weight can successfully modify the estimation in the IS method, even in high noise conditions.

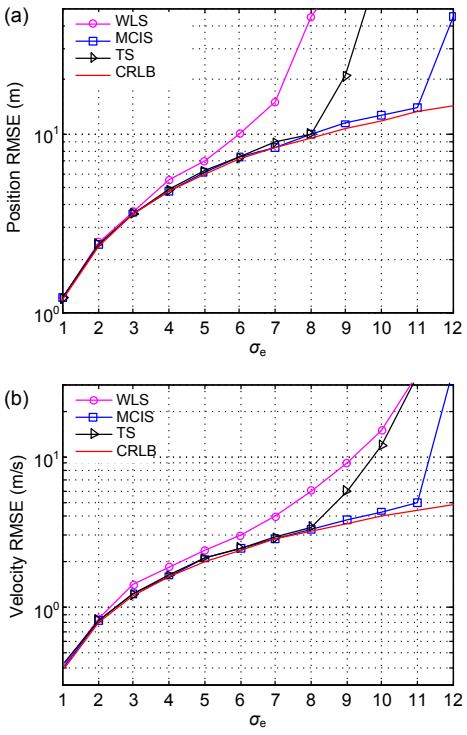

Fig. 2 RMSEs of the localization methods compared with the CRLB using four sensors in the 2D scenario when the position and velocity of the source are fixed: (a) RMSEs of source position estimates; (b) RMSEs of source velocity estimates

To examine the universality of the proposed method, we assume the exact position and the velocity of the emitter distributed randomly in the 600×600 and 60×60 square regions, respectively. The simulation results are shown in Fig. 3a for position estimates and Fig. 3b for velocity estimates. The WLS method performs much worse and is the first to exhibit a 'nonlinear threshold phenomenon'. The threshold effect occurs later in the TS method. The MCIS method shows performance that is superior to those of the other two methods and its performance degrades significantly until σ_e rises to 11.

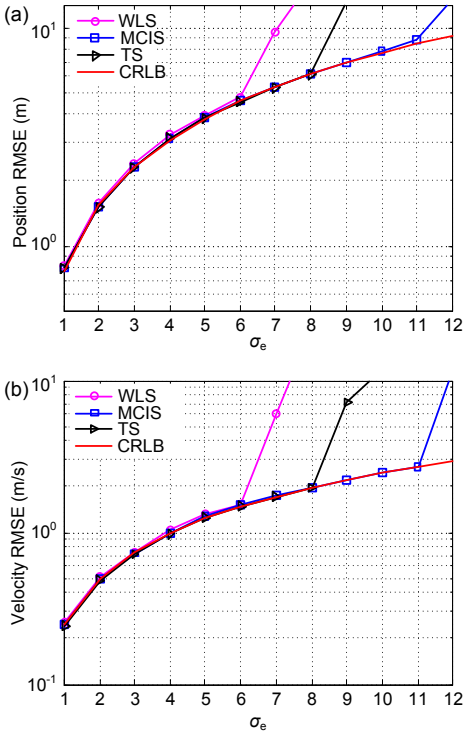

Fig. 3 RMSEs of the localization methods compared with the CRLB using four sensors in the 2D scenario when the source is located at a determinate square: (a) RMSEs of source position estimates; (b) RMSEs of source velocity estimates

Third, we examine the robustness of the proposed method to the non-ideal sensor localization geometry where four sensors locate in a line at (−300, −300), (−100, −100), (100, 100), and (300, 300), respectively. Figs. 4a and 4b show the simulated RMSEs of position and velocity estimates, respectively, when the source is located at (600, −50) with velocity (−30, 15). In this simulation, the WLS method fails to estimate the source position (its

RMSEs are not shown). The RMSEs of the TS method diverge from the CRLBs early in both position and velocity estimates and the MCIS method fails to converge only when σ_e>11, illustrating that the MCIS method can achieve better performance even with unsatisfactory sensor localization geometry.

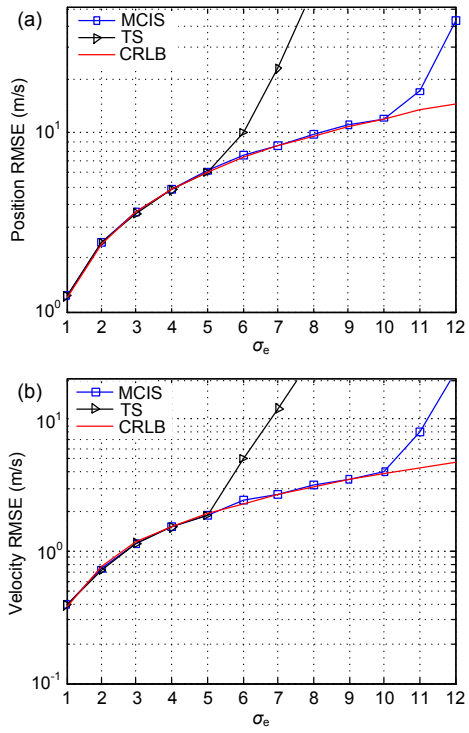

Fig. 4 RMSEs of the localization methods compared with the CRLB using four sensors located in a line in the 2D scenario: (a) RMSEs of source position estimates; (b) RMSEs of source velocity estimates

4.2.2 Three-dimensional scenario

We examine the performance of the proposed method in a 3D scenario where four sensors are used. The sensor positions and velocities are listed in Table 3. The source is located at (600, −150, 100) with velocity (−30, 15, 20). Other simulation settings are the same as in Section 4.2.1. Figs. 5a and 5b depict the RMSEs of position and velocity estimates, respectively. As shown, the MCIS method performs better than the other two methods and does not diverge until σ_e>10, where both the WLS and TS methods fail to converge. The proposed method, however, almost achieves CRLB.

Table 3 Positions and velocities of sensors in the 3D scenario

Sensor index	Sensor position (m)			Sensor velocity (m/s)		
	x	y	z	v_x	v_y	v_z
1	−300	200	−200	10	−10	10
2	300	−200	200	20	10	−10
3	300	200	−200	−10	20	−20
4	−300	−200	200	15	−15	15

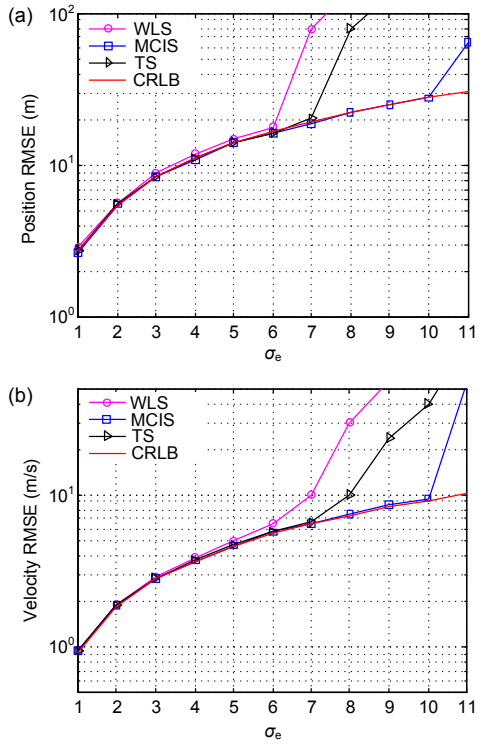

Fig. 5 RMSEs of the localization methods compared with the CRLB using four sensors in the 3D scenario when the position and velocity of the source are fixed: (a) RMSEs of source position estimates; (b) RMSEs of source velocity estimates

4.3 Sensitivity of MCIS to the initial estimate

The sensitivity of the MCIS method to the initial estimate is demonstrated here. We consider a 2D scenario with the same simulation conditions as in Section 4.2. We assume that the exact position and velocity of the emitter are unknown but are distributed randomly around the true position and velocity. Thus, we choose the initial estimate position $\boldsymbol{x}^*$ as $\boldsymbol{x}^*=\boldsymbol{x}+\boldsymbol{\Delta}$ and velocity $\dot{\boldsymbol{x}}^*$ as $\dot{\boldsymbol{x}}^*=\dot{\boldsymbol{x}}+0.1\boldsymbol{\Delta}$, where $\boldsymbol{\Delta}$ represents the initial estimate error and is submitted to zero-mean Gaussian distribution with covariance ϕ varying from 0 to 100 with an interval of 10. The

measurement error level is equivalent to 1. Meanwhile, we set the measurement noise level to σ_e=0.01. The simulations are based on 1000 Monte Carlo runs. Fig. 6 shows the RMSEs versus ϕ of the MCIS method where the source is located at (600, −50) with velocity (−10, 15). One can see that the TS and MCIS methods perform comparably at a low initial estimate error, but the RMSE of the TS method ascends rapidly with increasing ϕ. The RMSE of the proposed method ascends more slowly than that of the TS method; however, it is still mildly sensitive to high noise levels. To solve this problem, repetition of MCIS estimation can be employed. The RMSEs of both position and velocity estimates tend to become steady with multiple repetitions and the proposed method provides superior performance after two repetitions. This robustness of the MCIS method is derived from the importance sampling technique, which generates a series of samples based on a definite PDF and computes the weighted average according to the importance weights. Therefore, the global optimum can be attained and the influence of the initial estimated error is alleviated.

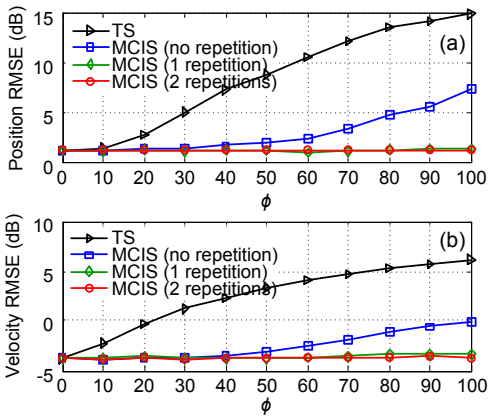

Fig. 6 Sensitivities of the estimation methods to the initial estimate errors in the 2D scenario when the position and velocity of the source are fixed: (a) RMSEs of the position estimates; (b) RMSEs of the velocity estimates

4.4 Influence of the number of sensors

Here we concentrate on the effect of the number of sensors. Consider a 2D scenario where sensors are arranged in a circle with a 500-m radius and their velocity vectors are arranged in a circle with a 40 m/s radius. We fix the measurement noise level σ_e=0.01 and perform 1000 Monte Carlo runs. The simulation results are shown in Fig. 7, where the number of sensors varies from 2 to 10. It is obvious that the WLS method performs much worse than the other methods and fails to localize with only two sensors. The TS method can give an ambiguous estimate of the position and velocity with a limited number of sensors and approximate the CRLB with a sufficient number of sensors. The MCIS method easily achieves the CRLB with only two sensors and performs better than the WLS and TS methods. One can conclude that the MCIS method can achieve a higher estimation accuracy with a limited number of sensors and the previous analysis is certified reasonably.

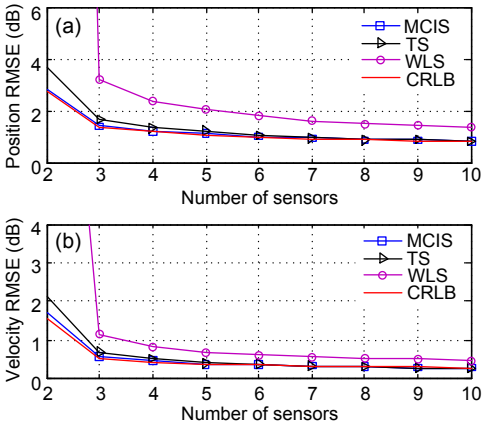

Fig. 7 Sensitivities of the estimation methods to the number of sensors used in the 2D scenario when the position and velocity of the source are fixed: (a) RMSEs of the position estimates; (b) RMSEs of the velocity estimates

5 Conclusions

This paper has demonstrated a high accuracy and low complexity localization algorithm for passive source localization based on TOA and FOA measurements. The Pincus theorem was used to obtain the global optimum of a nonlinear and nonconvex maximum likelihood problem by a multi-dimensional integral, which can be calculated efficiently using the Monte Carlo importance sampling (MCIS) method. We constructed a Gaussian distributed probability density function (PDF) as the importance function, which powerfully approaches the PDF of the target function and conveniently generates the samples. Furthermore, the global optimum can be attained by the correction of the importance weight. Simulation

results showed that the proposed method can achieve the CRLB for Gaussian noise at moderate noise levels and is excellently robust to the initial guess, especially when a few repetitions are performed. Moreover, the MCIS method significantly decreases the computational cost and outperforms the existing method with fewer available sensors.

References

Alizadeh, F., Goldfarb, D., 2003. Second-order cone programming. *Math. Prog.*, **95**(1):3-51. https://doi.org/10.1007/s10107-002-0339-5

Beck, A., Stoica, P., Li, J., 2008. Exact and approximate solutions of source localization problems. *IEEE Trans. Signal Process.*, **56**(5):1770-1778. https://doi.org/10.1109/TSP.2012.2191778

Broyden, C.G., 1970. The convergence of a class of double-rank minimization algorithms 1: general considerations. *IMA J. Appl. Math.*, **6**(1):76-90. https://doi.org/10.1093/imamat/6.1.76

Chan, Y.T., Hang, H.Y.C., Ching, P.C., 2006. Exact and approximate maximum likelihood localization algorithms. **55**(1):10-16. https://doi.org/10.1109/TVT.2005.861162

Cheung, K.W., So, H.C., Ma, W.K., *et al.*, 2004. Least squares algorithms for time-of-arrival-based mobile location. *IEEE Trans. Signal Process.*, **52**(4):1121-1130. https://doi.org/10.1109/TSP.2004.823465

Coleman, T.F., Li, Y., An, I., 2006. Trust region approach for nonlinear minimization subject to bounds. *SIAM J. Optim.*, **6**(2):418-445. https://doi.org/10.1137/0806023

Dong, L., 2012. Cooperative localization and tracking of mobile ad hoc networks. *IEEE Trans. Signal Process.*, **60**(7):3907-3913. https://doi.org/10.1109/TSP.2012.2191778

Elvira, V., Martino, L., Luengo, D., *et al.*, 2016. Heretical multiple importance sampling. *IEEE Signal Process. Lett.*, **23**(10):1474-1478. https://doi.org/10.1109/LSP.2016.2600678

Engel, U., 2009. A geolocation method using TOA and FOA measurements. positioning, navigation and communication. IEEE Workshop on Positioning, p.77-82. https://doi.org/10.1109/WPNC.2009.4907807

Fletcher, R., Reeves, C.M., 1964. Function minimization by conjugate gradients. *Comput. J.*, **7**(2):149-154. https://doi.org/10.1090/S0025.5718.1970.0274029.X

Foy, W.H., 1976. Position-location solutions by Taylor-series estimation. *IEEE Trans. Aerosp. Electron. Syst.*, **AES-12**(2):187-194. https://doi.org/10.1109/TAES.1976.308294

Fu, Z., Sun, X., Liu, Q., *et al.*, 2015. Achieving efficient cloud search services: multi-keyword ranked search over encrypted cloud data supporting parallel computing. *IEICE Trans. Commun.*, **98**(1):190-200. https://doi.org/10.1109/TSP.2012.2191778

Gu, B., Sun, X., Sheng, V.S., 2017. Structural minimax probability machine. *IEEE Trans. Neur. Netw. Learn. Syst.*, **28**(7):1646-1656. https://doi.org/10.1109/TNNLS.2016.2544779

Huang, J.G., Xie, D., Li, X., *et al.*, 2006. Maximum likelihood DOA estimator based on importance sampling. IEEE Region 10 Conf., p.1-4. https://doi.org/10.1109/TENCON.2006.344051

Kay, S.M., 1993. Fundamentals of Statistical Signal Processing, Volume I: Estimation Theory. Prentice-Hall, London, p.111-136.

Kay, S.M, 2006. Intuitive Probability and Random Processes Using MATLAB. Springer, Berlin. https://doi.org/10.1007/b104645

Knapp, C., Carter, G., 1976. The generalized correlation method for estimation of time delay. *IEEE Trans. Acoust. Speech Signal Process.*, **24**(4):320-327. https://doi.org/10.1109/TASSP.1976.1162830

Ma, Z., Ho, K.C., 2011. TOA localization in the presence of random sensor position errors. IEEE Int. Conf. on Acoustics, Speech and Signal Processing, p.2468-2471. https://doi.org/10.1109/ICASSP.2011.5946984

Masmoudi, A., Bellili, F., Affes, S., *et al.*, 2013. A maximum likelihood time delay estimator in a multipath environment using importance sampling. *IEEE Trans. Signal Process.*, **61**(1):182-193. https://doi.org/10.1109/TSP.2012.2222402

Pan, Z., Lei, J., Zhang, Y., *et al.*, 2016. Fast motion estimation based on content property for low-complexity H.265/HEVC encoder. *IEEE Trans. Broadcast.*, **62**(3):1-10. https://doi.org/10.1109/TBC.2016.2580920

Papakonstantinou, K., Slock, D., 2009. Hybrid TOA/AOD/Doppler-shift localization algorithm for NLOS environments. Int. Symp. on Personal, Indoor and Mobile Radio Communications, p.1948-1952. https://doi.org/10.1109/PIMRC.2009.5450008

Patwari, N., Ash, J.N., Kyperountas, S., *et al*., 2005. Locating the nodes: cooperative localization in wireless sensor networks. *IEEE Signal Process. Mag.*, **22**(4):54-69. https://doi.org/10.1109/MSP.2005.1458287

Pincus, M., 1968. A closed form solution of certain programming problems. *Oper. Res.*, **16**(3):690-694. https://doi.org/10.1287/opre.16.3.690

Ramlall, R., Chen, J., Swindlehurst, A.L., 2014. Non-line-of-sight mobile station positioning algorithm using TOA, AOA, and Doppler-shift. Ubiquitous Positioning Indoor Navigation and Location Based Service, p.180-184. https://doi.org/10.1109/UPINLBS.2014.7033726

Rappaport, T.S., Reed, J.H., Woerner, B.D., 1996. Position location using wireless communications on highways of the future. *IEEE Commun. Mag.*, **34**(10):33-41. https://doi.org/10.1109/35.544321

Shanno, D.F., 1970. Conditioning of quasi-Newton methods for function minimization. *Math. Comput.*, **24**(111):647-656. https://doi.org/10.1090/S0025.5718.1970.0274029.X

Shen, J., Molisch, A.F., Salmi, J., 2012. Accurate passive location estimation using TOA measurements. *IEEE Trans. Wirel. Commun.*, **11**(6):2182-2192. https://doi.org/10.1109/TWC.2012.040412.110697

Shikur, B.Y., Weber, T., 2014. Localization in NLOS environments using TOA, AOD, and Doppler-shift. 11th Workshop on Positioning, Navigation and Communication, p.1-6. https://doi.org/10.1109/WPNC.2014.6843297

Vandenberghe, L., Boyd, S., 1998. Semidefinite programming. *SIAM Rev.*, **38**(1):49-95. https://doi.org/10.1137/1038003

Wang, G., Chen, H., 2011. An importance sampling method for TDOA-based source localization. *IEEE Trans. Wirel. Commun.*, **10**(5):1560-1568. https://doi.org/10.1109/TWC.2011.030311.101011

Wang, H., Kay, S., 2010. Maximum likelihood angle-Doppler estimator using importance sampling. *IEEE Trans. Aerosp. Electron. Syst.*, **46**(2):610-622. https://doi.org/10.1109/TAES.2010.5461644

Wang, H., Kay, S., Saha, S., 2008. An importance sampling maximum likelihood direction of arrival estimator. *IEEE Trans. Signal Process.*, **56**(10):5082-5092. https://doi.org/10.1109/TSP.2008.928504

Wang, Y., Wu, Y., 2015. An improved direct position determination algorithm with combined time delay and Doppler. *J. Xi'an Jiaotong Univ.*, **49**(4):123-129. https://doi.org/10.7652/xjtuxb201504020

Wang, Y., Wu, Y., 2016. An efficient semidefinite relaxation algorithm for moving source localization using TDOA and FDOA measurements. *IEEE Commun. Lett.*, **21**(1):80-83. https://doi.org/10.1109/LCOMM.2016.2614936

Weiss, A.J., 2003. On the accuracy of a cellular location system based on RSS measurements. *IEEE Trans. Veh. Technol.*, **52**(6):1508-1518. https://doi.org/10.1109/TVT.2003.819613

Xia, Z., Wang, X., Zhang, L., *et al.*, 2016. A privacy-preserving and copy-deterrence content-based image retrieval scheme in cloud computing. *IEEE Trans. Inform. Forens. Secur.*, **11**(11):2594-2608. https://doi.org/10.1109/TSP.2012.2191778

Yin, J.X., Wu, Y., Wang, D., 2014. On 2-D direction-of-arrival estimation performance for rank reduction estimator in presence of unexpected modeling errors. *Circ. Syst. Signal Process.*, **33**(2):515-547. https://doi.org/10.1007/s00034-013-9654-8

Yin, J.X., Wu, Y., Wang, D., 2016. An auto-calibration method for spatially and temporally correlated noncircular sources in unknown noise fields. *Multidimens. Syst. Signal Process.*, **27**(2):1-29. https://doi.org/10.1007/s11045-015-0316-9

Zhang, W., Zhang, G., 2011. An efficient algorithm for TDOA/FDOA estimation based on approximate coherent accumulative of short-time CAF. Int. Conf. on Wireless Communications and Signal Processing, p.1-4. https://doi.org/10.1109/WCSP.2011.6096807